Efficient Tracking of Heart Rate under Physical Exercise from Photoplethysmographic Signals

Conference Paper · September 2015

DOI: 10.1109/RTSI.2015.7325116

7 authors, including:

Guglielmo Frigo
Federal Institute of Metrology (METAS)
60 PUBLICATIONS **374** CITATIONS
SEE PROFILE

Marco Fabris
Technion - Israel Institute of Technology
5 PUBLICATIONS **6** CITATIONS
SEE PROFILE

Italo Agustin Marsili
Università degli Studi di Trento
5 PUBLICATIONS **12** CITATIONS
SEE PROFILE

Claudio Narduzzi
University of Padova
120 PUBLICATIONS **1,109** CITATIONS
SEE PROFILE

Efficient Tracking of Heart Rate under Physical Exercise from Photoplethysmographic Signals

G. Frigo, M. Fabris, A. Galli, F. Gambarin, I. A. Marsili, C. Narduzzi and G. Giorgi
Department of Information Engineering
University of Padua
via G. Gradenigo, 6/b, I-35131 Padova, Italy

***Abstract*— This paper deals with the estimation of the temporal evolution of heart rate (HR), in subjects undertaking physical exercise, using wrist-type photoplethysmographic (PPG) signals. The proposed algorithm employs a zero-padded DFT to provide a raw HR estimate with small frequency granularity and feeds it into a Kalman filter to accurately track HR evolution over time. Furthermore, heuristics are applied to sort out the estimates provided by spectral analysis and determine a reasonable preliminary frequency value.**

The algorithm was an entrant into the 2015 Signal Processing Cup [1] and has been tested, with very encouraging results, on the set of recorded waveforms (training traces) provided for that competition. In this paper we discuss its features and outline possible improvements. Measurement results on actual recorded traces are given and are shown to outperform those provided in [2] on all training traces provided for the competition.

I. Introduction

Photoplethysmography is an optical technique that detects the changes in blood volume occurring in tissues at the microvascular level. It allows simple, low-cost non-invasive measurements at the skin surface, providing physiological parameters like oxygen saturation, blood pressure and heart-beat rate [3]. A photoplethysmographic (PPG) signal is obtained by illuminating the subject skin using a light-emitting diode (LED) and measuring the changes in the intensity of light reflected from the skin. The resulting waveform is composed of a pseudo-periodic pulse component, attributed to changes in blood volume occurring with each heart beat, with components related to respiration, nervous activity and thermoregulation superimposed on it [4].

PPG technology is widely used in commercially available medical devices and, since the periodicity of the PPG signal corresponds to the cardiac rhythm, it is also a candidate for heart rate (HR) monitoring during physical exercise [5]. Although its low cost and ease of application are attractive, estimation of heart-beat rate from PPG signals is notoriously hard to achieve when subjects are performing physical activities [6]. As noted, for instance, in [2], [7] motion artifact (MA) in PPG signals may be significant and cause any estimation algorithm to focus on a wrong signal component.

The algorithm presented in this paper combines spectral analysis obtained by a Discrete Fourier Transform (DFT), zero-padded to achieve better frequency granularity, with a Kalman filter (KF) which is used to track HR temporal evolution. Furthermore, the KF performs an acceptance test on new measurements, that are compared with a threshold based on the variance of the KF innovation process. Whenever the innovation value exceeds the threshold, the new measurement is discarded and the value predicted by the state equations is kept instead as the new heart-beat rate estimate.

In between, some heuristics are also applied to sort out the estimates provided by spectral analysis and determine a reasonable frequency value. Heuristics are based on some empirical assumptions regarding admissible values for the human heart beat rate. These values are extensively used for checking the validity of the estimates obtained from spectral analysis of the PPG signals and also to avoid tracking of false peak values by the Kalman filter. Therefore, their initial setting is very important and represents a crucial aspect of the proposed algorithm. Parameters have been mainly derived from an empirical study on the training traces provided for the 2015 Signal Processing Cup competition [1].

II. Process and measurement model

In the following we model the human heart rate evolution by a couple of finite-difference equations:

$$\begin{cases} \theta(k) &= \theta(k-1) + \gamma(k-1)\Delta T + \omega_\theta(k) \\ \gamma(k) &= \gamma(k-1) + \omega_\gamma(k) \end{cases} \tag{1}$$

where $\theta(k)$ and $\gamma(k)$ represent respectively the HR value and the HR first derivative at the k-th time instant; in the same way $\theta(k-1)$ and $\gamma(k-1)$ represent the same quantities at the $(k-1)$-th time instant. $\omega_\theta(k)$ and $\omega_\gamma(k)$ are two zero-mean gaussian-distributed random processes representing respectively white noise and random walk noise in the HR model. Equations describing the temporal evolution of the heart rate and the measurement process are summarized in vector-matrix form as:

$$\mathbf{x}(k) = \mathbf{A}\mathbf{x}(k-1) + \mathbf{w}(k) \tag{2}$$

$$z(k) = \mathbf{H}\mathbf{x}(k) + v(k). \tag{3}$$

The first equation describes the evolution of the process, which depends on the state vector $\mathbf{x}(k) = [\theta(k)\ \gamma(k)]^T$, and on the state transition matrix:

$$\mathbf{A} = \begin{bmatrix} 1 & \Delta T \\ 0 & 1 \end{bmatrix} \tag{4}$$

978-1-4673-8167-3/15/$31.00 ©2015 IEEE

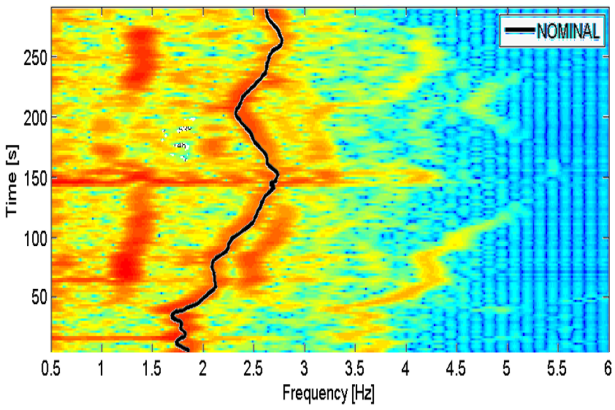

Fig. 1. Spectrogram calculated from raw PPG measurements compared with ECG reference value (black line). Spectrogram has been calculated by considering overlapping time windows of 8 seconds. Adjacent windows have an overlap of 6 seconds, as explain in Sec.IV. An RGB colormap is used for representing amplitude information, where blue is associated values of low amplitude while instead red is used for representing components of high intensity.

The vector $\mathbf{w}(k) = [\omega_\theta(k)\ \omega_\gamma(k)]^T$ represents process noise.

The second equation represents the measurement process during which a raw HR estimate: $z(k) = \hat{\theta}(k)$ is obtained by spectral analysis, as will be discussed in the following. Finally, $v(k) = \hat{v}_\theta(k)$ is the measurement noise vector and the matrix $\mathbf{H} = [1\ 0]$ is the corresponding measurement matrix.

III. Data Set Features

The trace library on which the algorithm has been developed provides a comprehensive set of test cases that covers subjects of various ages undertaking physical exercises of different intensity. Each trace includes PPG recordings from two pulse oximeters and a triaxial accelerometer, that were carried within a wristband. Furthermore, ground truth data are included in the form of a simultaneously recorded electrocardiographic (EGC) trace. All signals were acquired with a sampling frequency $F_S = 125\ Hz$.

Signals were acquired, as described in [2], during physical activity on a treadmill with changing speeds. In particular during the first 30 s of acquisition the subject lies still, then it runs for 60 s at a speed of 8 km/h, successively the speed is increased to 15 km/h for a period of 60 s and finally decreased at the initial value of 8 km/h for others 60 s. The test stops with a final rest break of 30 s. Overall, each test lasts about 300 seconds.

The HR varies in accordance with physical stress, even though in a manner that strictly depends on the physical conditions of a subject. In Fig. 1 the spectrogram obtained from a raw PPG signal -corresponding to subject 6, as explained in the following- has been reported in comparison with the reference signal solid black line) extracted from ECG measurements. As it can be noted, HR varies in the range between 1.5Hz and 3Hz, corresponding respectively to 90 bpm and 180 bpm. By examining the spectrogram, we can see that peak values (corresponding to red area) are not univocally associated to the frequency corresponding to heart rate due to the presence of motion artifacts that give rise to a more complex frequency response. The solution adopted in this paper, for correctly estimated HR despite the presence of MAs of strong magnitude, is based on a tracking algorithm, that has to be correctly initialized during an initial training phase. The assumption is that the PPG signal acquired during such training phase is unaffected by the presence of MAs. Usually the training phase corresponds about to the first 30 seconds of acquisition, during which the subject is not in motion and therefore the highest peak in frequency of PPG signal corresponds to the cardiac rhythm, as can be noted in Fig.1.

IV. Frequency analysis of PPG signals

Achieving HR resolution of less than one beat per minute (1 bpm) was among the performance targets and it should be noted that the requirement translates into the need to detect a minimum frequency shift $\Delta_f < \frac{1}{60}$ Hz. For a plain DFT, working on a frequency grid with such a fine step would require calculation over a time window of at least of 60 s and a consequent record length of at least 7500 samples.

Zero padding allows to obtain a fine grid step with much shorter data sequences. However, while the frequency grid step is the reciprocal of the length of the zero-padded sequence, resolution is inversely proportional to the length of the (shorter) actual sample sequence. Of course, this places a more severe limit on the capability to resolve different but closely spaced frequency components. Nevertheless, frequency components in PPG signals are mostly separated well enough that they can usually be resolved. Component frequencies do change according to the type and intensity of physical exercise, so that the frequency of an MA component may get close to the HR frequency, but in this case tracking by the KF helps discriminate the outlier component.

Consequently, DFT is evaluated on $M > N$ samples by using a zero-padding operation: the first N-samples correspond to the vector $\mathbf{x}(i) = [x(i), x(i-1), \ldots, x(i-N+1)]$, while the subsequent $M - N$ values are nil. The zero-padded DFT operator will be indicated by: $DFT(\mathbf{x}, N, M)$. Currently, vector length is set to $N = 1000$ samples, corresponding to an observation window length $T_W = 8$ s. Consecutive windows have a 75% overlap (that is, 6 s), so that the algorithm provides a new HR estimate every $T_{output} = 2\ s$, corresponding to a final reporting rate $F_{output} = 0.5\ Hz$.

V. Algorithm description

The proposed algorithm has been developed in Matlab^{TM}. It is based on an initial **training stage**, during which the Kalman filter is properly initialized, followed by a **main loop** that takes sensor measurements over fixed-duration overlapping windows

from a given measurement trace and processes acquired data to provide an accurate estimate of the actual heart rate value in bpm.

An iteration of the main loop consists in:

- a **prediction stage**, where *a-priori* estimates are obtained both for the HR value and its variance;
- a **raw HR estimation stage**, where a raw value for the HR is obtained by a zero-padded DFT on a given time window
- and an **update stage**, where a refined *a-posteriori* HR estimate and its variance are provided.

A description of these steps is provided in the following.

A. Training stage

The basic assumption for the validity of results provided at the end of the training stage is that during the starting measurement period, sensor data provided by the two PPG sensors, indicated respectively by $x_{PPG,1}$ and $x_{PPG,2}$, are almost free of motion artifacts.

The first operation consists in applying a band-pass digital filter on the raw PPG values provided at the sensor output, obtaining the filtered signal[1] $x_{f,PPG}$. The low and high frequency cutoff values have been set, considering the range of admissible human HR values, to: $f_{BP,low} = 0.33\ Hz$ and $f_{BP,high} = 3.17\ Hz$.

The spectrum of the filtered PPG signal is then estimated by a zero-padded DFT:

$$X_{f,PPG}(k\Delta_f) = DFT\left(\mathbf{x}_{PPG}, N, M\right) \tag{5}$$

where $0 \leq k\Delta_f \leq F_S$. F_S and F are respectively the sensor sampling frequency and the frequency resolution. This latter depends on the number of samples used for calculating the DFT: $F = \frac{F_S}{M}$.

The initial HR estimate is finally obtained by considering the index of the peak value:

$$k_{peak} = \arg\max_k |X_{f,PPG}(k\Delta_f)| \tag{6}$$

where the possible range of values for k is chosen to fall within the range $f_{BP,low} \leq k\Delta_f \leq f_{BP,high}$. Of course, the resulting frequency estimate is $k_{peak}\Delta_f$. Initially, $f_{BP,low}$ and $f_{BP,high}$ are set in accordance with physiological parameters.

B. Main loop

1) KF Prediction stage: As previously mentioned, the Kalman filter operates in two stages. In the first stage, called **prediction stage**, the *a priori* estimate is obtained from the knowledge of the state at the previous time instant $k-1$:

$$\hat{\mathbf{x}}^-(k) = \mathbf{A}\mathbf{x}^+(k-1) \tag{7}$$

$$\mathbf{P}^-(k) = \mathbf{A}\mathbf{P}^+(k-1)\mathbf{A}^T + \mathbf{Q} \tag{8}$$

[1]When no ambiguity arises, we just use the notation x_{PPG} for the signal provided by any given PPG sensor.

where $\hat{x}^-(k)$ is the *a priori* state estimate. $\mathbf{P}^-(k)$ is the 2×2 *a priori* estimate error covariance matrix which can be determined by the *a posteriori* estimate error covariance $\mathbf{P}(k-1)$ and the process noise covariance matrix $\mathbf{Q}$, which is initialized by considering the variances of the process noise components: $\mathbf{Q} = \text{diag}\left\{\text{var}[\omega_\theta], \text{var}[\omega_\gamma]\right\}$.

The HR frequency value is expected to fall within the confidence interval:

$$\left[\theta^-(k) - \kappa_\alpha\sqrt{P^-_{1,1}(k)},\quad \theta^-(k) + \kappa_\alpha\sqrt{P^-_{1,1}(k)}\right] \tag{9}$$

with a given probability that depends on the coverage factor κ_α, that must be carefully chosen. The value $\theta^-(k)$ corresponds to the first element of the *a priori* state estimate vector $\mathbf{x}^-(k) = [\theta^-(k), \gamma^-(k)]$, while $P^-_{1,1}(k)$ is the first element on the diagonal of the *a priori* state error covariance matrix $\mathbf{P}^-(k)$.

2) Raw HR estimation: Measurements $z(k)$ used in the Kalman filter are obtained by spectral analysis, as previously described for the training stage. In this case however, sensor signals are usually also affected by impairments due to motion artifacts that need to be taken into account.

Our approach makes use of information provided by the Kalman filter for establishing an admissible range of frequencies, where the peak associated to the HR signal is expected to lie. In particular the peak of the estimated spectrum $|X_{PPG}(k\Delta_f)|$, calculated by a zero-padded DFT as previously described, is now searched within the interval of values $f_{low} \leq k\Delta_f \leq f_{high}$, where:

$$f_{low} = \theta^-(k) - \min\left[\tau_\sigma,\ \kappa_\alpha \cdot \sqrt{P^-_{1,1}(k)}\right] \tag{10}$$

and

$$f_{high} = \theta^-(k) + \min\left[\tau_\sigma,\ \kappa_\alpha \cdot \sqrt{P^-_{1,1}(k)}\right] \tag{11}$$

It can be seen that, to avoid any divergent behavior for the Kalman filter, the low and upper frequency threshold values are further bounded using the physiologic limit τ_σ, which represents the maximum HR frequency deviation that may take place during time interval T_{output}.

The same analysis is done for estimates from both sensors, PPG1 and PPG2. In order to discriminate measurement outliers from actual values due to particular physical conditions, for instance associated to a stress or relax phase of the subject under analysis, the values obtained for PPG1 and PPG2 are compared with each other. If they are comparable then the measurement will be considered reliable, otherwise the measurement will be accepted only if the PPG1 estimated value is within the range of admissible values. Failing this, the measurement for the considered window will be flagged as not available and the *a priori* estimate will be provided instead.

Analysis of experimental data showed that a spectral peak corresponding to the second harmonic of the PPG signal can also be noticed. To improve the accuracy of the frequency estimate, when the measurement provided by PPG1 is considered acceptable the algorithm looks also for a second peak in the range between $f_{low}^{(2)}$ and $f_{high}^{(2)}$, where

$$f_{low}^{(2)} = 2\theta(k)^- - DPE \tag{12}$$

and

$$f_{high}^{(2)} = 2\theta(k)^- + DPE \tag{13}$$

and $DPE = \frac{3}{60}\ Hz$ is an empirically determined parameter. If the estimated value $f_{peak}^{(2)}$ results to be reliable, then we will halve this value and consider the new raw frequency measurement to be:

$$f_{peak} = \frac{f_{peak}^{(2)}}{2}. \tag{14}$$

Finally, if any error occurs during this stage the measurement will be flagged as unavailable.

3) KF Update stage: This consists in a **correction stage**, in which the *a posteriori* state estimate $\mathbf{x}^+(k)$ and the *a posteriori* covariance matrix $\mathbf{P}(k)$ are updated. If a new measurement is available, the first operation during the update stage consists in validating the measurement. This is done by considering the innovation contribution, that is, the difference between the raw measurement and the *a priori* estimate:

$$\mathbf{inn}(k) = z(k) - \mathbf{H}\hat{\mathbf{x}}^-(k) \tag{15}$$

and its covariance:

$$\mathbf{S}(k) = \mathbf{H}\mathbf{P}^{-1}(k)\mathbf{H}^T + \mathbf{R}, \tag{16}$$

where $\mathbf{R} = \text{var}[v]$ is the measurement noise variance. The new measurement is accepted only if the following condition is satisfied:

$$\mathbf{inn}(k) \leq \kappa_\beta \cdot \sqrt{\mathbf{S}(k)} \tag{17}$$

where κ_β is a factor associated to suitable confidence level.

If the condition is satisfied, Kalman filter variables are updated as follows:

$$\begin{aligned} \mathbf{K}(k) &= \mathbf{P}^-(k)\mathbf{H}^T\mathbf{S}(k)^{-1} \\ \mathbf{x}^+(k) &= \hat{\mathbf{x}}^-(k) + \mathbf{K}(k)\cdot\mathbf{inn}(k) \\ \mathbf{P}^+(k) &= (\mathbf{I} - \mathbf{K}(k)\mathbf{H})\,\mathbf{P}^-(k) \end{aligned} \tag{18}$$

where $\mathbf{K}(k)$ is the Kalman gain that can be calculated as follow:

$$\mathbf{K}(k) = \frac{\mathbf{P}^-(k)\mathbf{H}^T}{\mathbf{H}\mathbf{P}^-(k)\mathbf{H}^T + \mathbf{R}} \tag{19}$$

Otherwise, if no measurement is available or if the measurement is flagged as unreliable, the *a posteriori* quantities remain unchanged:

$$\begin{aligned} \mathbf{x}^+(k) &= \hat{\mathbf{x}}^-(k) \\ \mathbf{P}^+(k) &= \mathbf{P}^-(k) \end{aligned} \tag{20}$$

The output value, at the end of the k-th iteration of the main loop, corresponds to the the first element of the *a posteriori* state estimation vector:

$$f_{out}(k) = \theta^+(k). \tag{21}$$

VI. Results

Results obtained with the proposed KF-based algorithm (named KF+DFT) are summarized in Tab. I and in Tab. II for a set of 12 traces, corresponding to 12 different subjects, and compared with the values published in [2], where a different algorithm is presented (indicated for simplicity as TROIKA). The comparison has been done by considering two different performance metrics:

- $Err_1 = \frac{1}{N}\sum_{n=1}^{N} |60 \times \theta(n)^+ - BPM_{true}(n)|$ in bpm, which corresponds to the average absolute error with respect to reference values represented by $BPM_{true}(n)$,
- $Err_2 = \frac{1}{N}\sum_{n=1}^{N} \frac{|60 \times \theta(n)^+ - BPM_{true}(n)|}{BPM_{true}(n)}$ in percentage, that represents the average percent error with respect to reference values.

In Fig. 2 results reported in Tab. I have been graphically compared. The target corresponding of an absolute error less than 1 bpm has been represented by a dashed red line. As can be noted, HR estimates obtained by the proposed algorithm show, on average, better agreement with the reference values obtained from the ECG trace, even though the target is met only in few cases. There are in particular some cases where the error results to be very large, as explain in more details in the following.

It is also important to consider pointwise accuracy of the algorithm, since occasional large deviations of HR estimates would make the algorithm output unreliable. For this reason, estimation results obtained for subjects 5, 6 and 10 have also been plotted over time, together with reference values, and are reported for comparison in Figs. 3-5. The reference value has been reported by a red line, raw measurements provided by a zero-padded DFT by black stars, while final estimated values by a blue line. With green lines the uncertainty interval obtained by considering the a-posteriori error covariance matrix is also provided.

It can be seen that the algorithm tracks the reference value fairly well, although occasional fluctuations may take place. These are often the consequence of the algorithm discarding some measurements, following the validation check defined by

TABLE I

AVERAGE ABSOLUTE ERROR (ERR 1) BETWEEN PROPOSED HEART-BEAT RATE ESTIMATES AND GIVEN REFERENCE VALUES.

# Trace	1	2	3	4	5	6	7	8	9	10	11	12
Err 1 (KF+DFT)	2.11	1.89	1.01	1.08	0.61	1.66	0.54	0.59	0.54	4.12	1.15	2.83
Err 1 (TROIKA)	2.29	2.19	2.00	2.15	2.01	2.76	1.67	1.93	1.86	4.70	1.72	2.84

TABLE II

AVERAGE PERCENT ERROR (ERR 2) BETWEEN PROPOSED HEART-BEAT RATE ESTIMATES AND GIVEN REFERENCE VALUES.

# Trace	1	2	3	4	5	6	7	8	9	10	11	12
Err 2 (KF+DFT)	1.71%	1.56%	0.88%	1.00%	0.46%	1.37%	0.42%	0.52%	0.48%	2.75%	0.74%	1.86%
Err 2 (TROIKA)	1.90%	1.87%	1.66%	1.82%	1.49%	2.25%	1.26%	1.62%	1.59%	2.93%	1.15%	1.99%

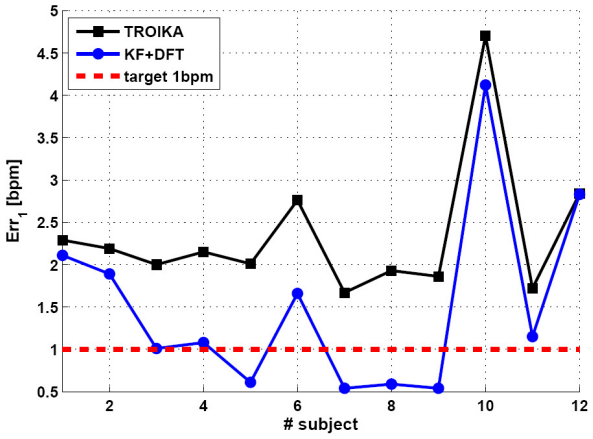

Fig. 2. Comparison of performances achievable by the proposed algorithm with respect to the algorithm discussed in [2].

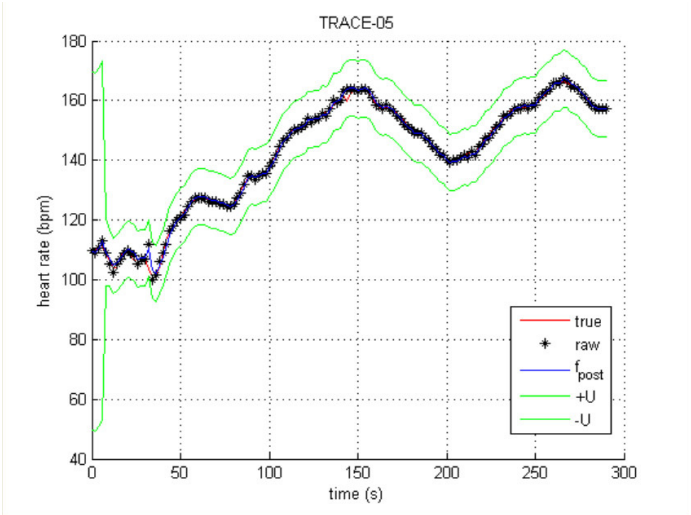

Fig. 3. Heart-beat rate estimation results on subject 5, expressed in beats per minute (bpm).

(17), as can be noted both in Fig. 4 and 5 in correspondence to when subjects start to run.

VII. CONCLUSIONS

The algorithm proposed in this work employs a Kalman filter to track the temporal evolution of the heart rate and a DFT with zero-padding for obtaining the raw measurement values. In terms of computational requirements it is, therefore, fairly lightweight compared to [2] and other algorithms mentioned within.

For instance, no preliminary denoising operation is performed to reduce the impact of MA components, except simple band-pass filtering. A good degree of robustness is still afforded by KF-based tracking, whose implementation is comparatively undemanding as far as computation is concerned.

We also tried to work on as few signals as possible, purposely avoiding the use of accelerometer data to detect potential MA outliers, as we targeted a low-cost implementation of the algorithm. In spite of this, when an MA component frequency gets close to the heart rate, so that spectral peaks tend to merge, the frequency error resulting from a raw peak search remains acceptable, if one considers that it will be further smoothed out by the KF.

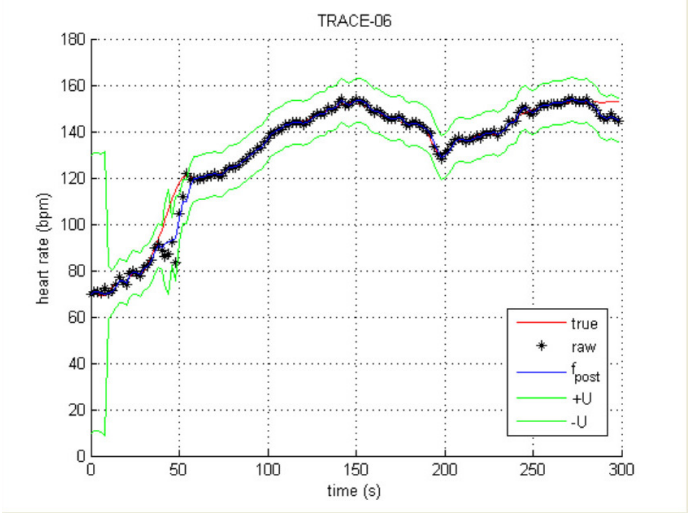

Fig. 4. Heart-beat rate estimation results on subject 6, expressed in beats per minute (bpm).

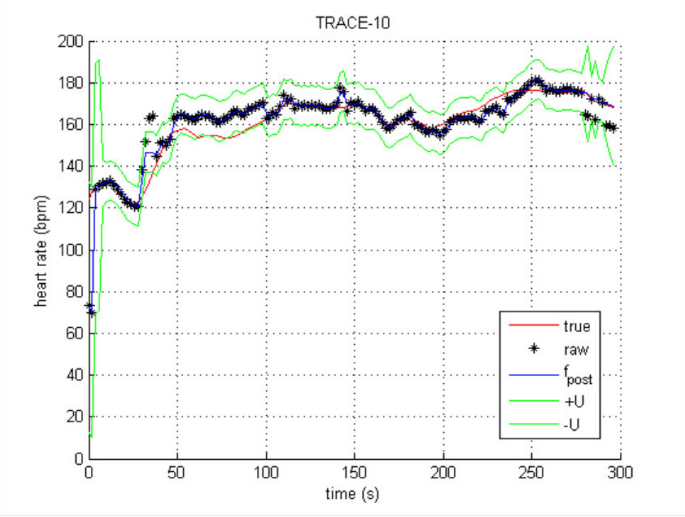

Fig. 5. Heart-beat rate estimation results on subject 10, expressed in beats per minute (bpm).

A fundamental point to consider is the very low execution time for the proposed algorithm. Furthermore, the algorithm is very simple and can be implemented on low-cost devices where memory and CPU availability also need to be considered as essential system requirements.

REFERENCES

[1] *IEEE Signal Processing Cup 2015*, available on line: http://www.signalprocessingsociety.org/community/sp-cup/

[2] Z. Zhang, Z. Pi and B. Liu, "TROIKA: a general framework for heart rate monitoring using wrist type photoplethysmographic signals during intensive physical exercise", *IEEE Trans. Biomed. Eng.*, vol. 62, no. 2, pp. 522-531, Feb. 2015.

[3] E. Gil et al., Photoplethysmography pulse rate variability as a surrogate measurement of heart rate variability during non-stationary conditions, *Physiol. Meas.*, vol. 31, no. 9, pp. 12711290, 2010.

[4] J. Allen, "Photoplethysmography and its application in clinical physiological measurement", *Physiol. Meas.*, 28 (2007), R1-R39.

[5] Xiaochuan He; Goubran, R.A.; Liu, X.P., "Secondary Peak Detection of PPG Signal for Continuous Cuffless Arterial Blood Pressure Measurement", *IEEE Trans. Instr. Meas.* , vol.63, no.6, pp.1431,1439, June 2014.

[6] Gil, E.; Laguna, P.; Martinez, J.P.; Barquero-Perez, O.; Garcia-Alberola, A.; Sornmo, L., "Heart Rate Turbulence Analysis Based on Photoplethysmography", *IEEE Trans. Biomed. Eng.*, vol.60, no.11, pp.3149,3155, Nov. 2013.

[7] B. S. Kim and S. K. Yoo, Motion artifact reduction in photoplethysmography using independent component analysis, *IEEE Trans. Biomed. Eng.*, vol. 53, no. 3, pp. 566568, 2006.